CONTRIBUTION TO THE ASSESSMENT OF SHELTER-IN-PLACE EFFECTIVENESS AS A COMMUNITY PROTECTION MEASURE IN THE EVENT OF A TOXIC GAS RELEASE

María Isabel Montoya Rodríguez

A dissertation submitted in partial satisfaction of the
requirements for the degree of:

Doctor by the Universitat Politècnica de Catalunya

Supervided by:
Dra. Eulàlia Planas Cuchi

CERTEC – Centre d'Estudis del Risc Tecnològic
Departament d'Enginyeria Química
Escola Tècnica Superior d' Enginyers Industrials de Barcelona
Universitat Politécnica de Catalunya

Barcelona, September 2010

4.3.1 Using geometric means of dwellings' characteristics by census tract

In this case we used the GM of floor area, year of construction and number of stories to represent each census tract, as in Figure 4.4 to Figure 4.6. Then, with these values and depending on the climate zone where it is located, we computed the *NL* for each census tract through Eq. 2.45. Figure 4.12 shows the results of the *NL* estimated, where it can be seen that most of the census tracts present values between 0.41 and 1.2, which are normal values of US dwellings (McWilliams & Jung, 2006). Higher values belong to the dry climate zone, while smaller values lied in the humid zone. This behavior is mainly influenced by the NL_{cz} coefficients of the model (see Table 2.8), which are very different; since others variables do not show a special behavior in these zones.

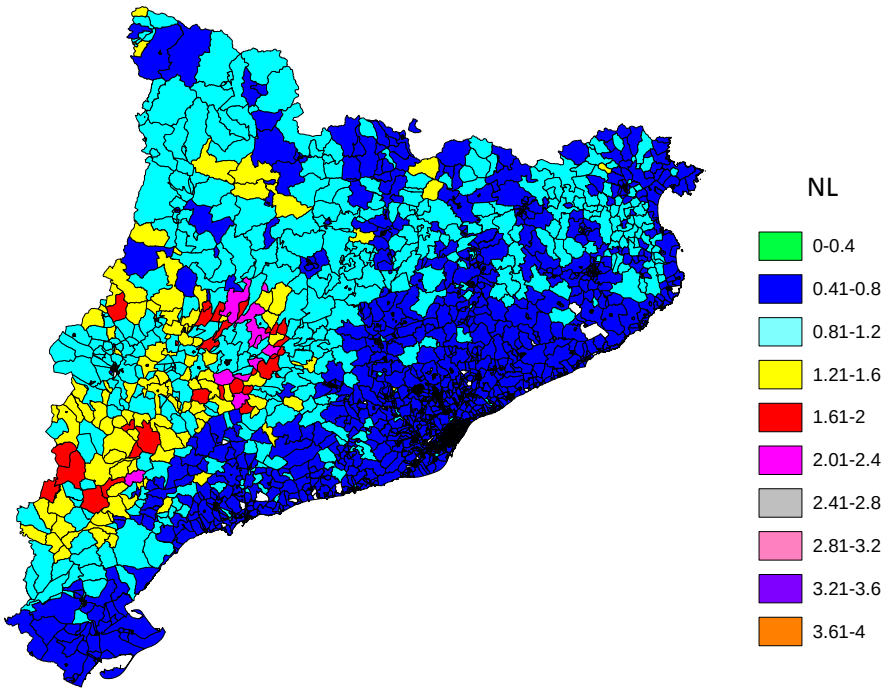

Figure 4.12 *NL* of single-family dwellings predicted using the geometric means of dwellings' characteristics by census tract

Computed the *NL*, the ELA was estimated from Eq. 4.1 (see Eq. 2.43), assuming a standard height of 2.5 m for each story.

$$ELA = 1 \cdot 10^{-3} \cdot NL \cdot Area \cdot \left(\frac{H}{H_o} \right)^{-0.3} \qquad \text{Eq. 4.1}$$

Figure 4.13 shows the results of *ELA* by census tract, from which it can be seen that *ELA* mainly range between 0.041 and 0.1650 m^2. As for the *NL*, the leakier region is the dry zone. However, the visual difference between the dry and humid regions in the *ELA* representation is not as visible as in the *NL*, due to the inclusion of the floor area and the height in the estimation of the *ELA*, which affects its value. The reference value in the French energy performance regulation, I_4, is 0.8 $m^3/(h \cdot m^2)$ (see Table 2.13). Therefore, assuming a house with a floor area of 100 m^2, a C_D of 1, ρ = 1.2 kg/m^3, and a V/S_f of 1.4 m^3/m^2, the corresponding *ELA* would be 0.0153 m^2, which is a small value if compared with those of the census tracts.

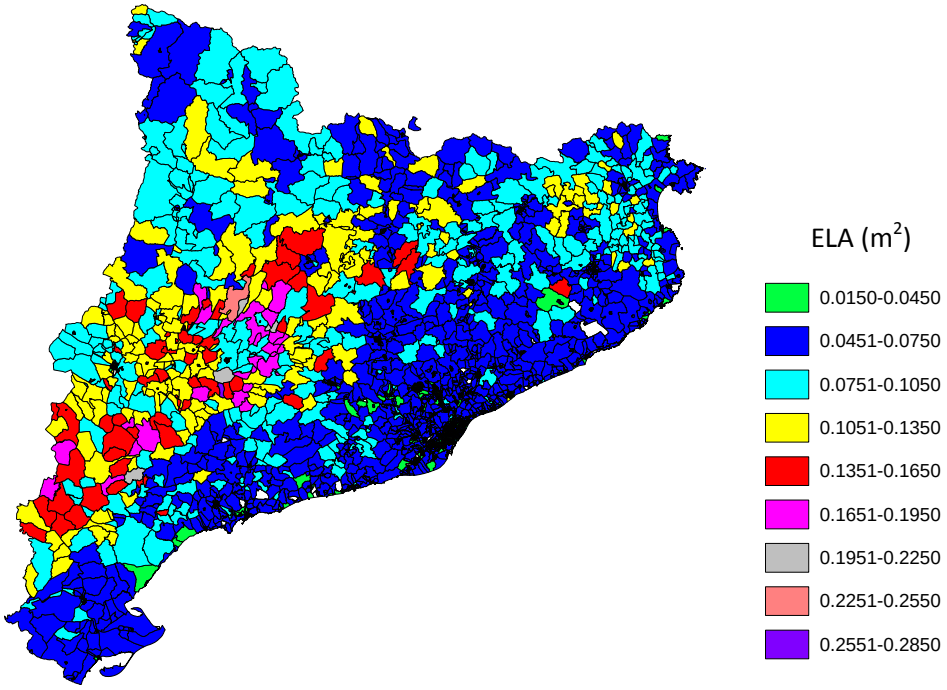

Figure 4.13 *ELA* of single-family dwellings predicted using the geometric means of dwellings' characteristics by census tract

ACH estimation

With the airtightness, the *ACH* can be estimated using the AIM-2 model described in section 2.4.2. To use this model, the airtightness must be expressed in terms of *c* and *N* of the power law (Eq. 2.40). Thereby, *N* was assumed as 2/3, which is a typical value of this variable, and *c* was estimated from Eq. 4.2 (see Eq. 2.43 and Eq. 2.44) using *NL*, a ΔP_r of 4 Pa (since this is the ΔP for which the *NL* is defined), a C_D of 1 and ρ = 1.2 kg/m^3 (air density at 1 atm and 293.15 K).

$$c = \frac{1 \cdot 10^{-3} \cdot NL \cdot Area \cdot C_D}{(\Delta P_r)^{N-0.5}} \cdot \left(\frac{H}{H_o}\right)^{-0.3} \cdot \sqrt{\frac{2}{\rho}} = \frac{ELA \cdot C_D}{(\Delta P_r)^{N-0.5}} \cdot \sqrt{\frac{2}{\rho}} \qquad \text{Eq. 4.2}$$

To apply the AIM-2 model, the following assumptions were also made:

- The presence of a flue was assumed for all dwellings, as this is a typical construction feature in single-family dwellings in Catalunya.
- Each story was 2.5 m high.
- The flue outlet was 1.5 m above the upper ceiling.
- Crawl space foundations were not considered. Single-family dwellings in Catalunya are typically constructed using heavy materials, and crawl spaces in this type of construction are very well insulated, so the potential air infiltration through this space is considered negligible.
- All infiltration was assumed to take place through the walls and the flue. Infiltration through floor and ceiling was not considered, since the techniques and materials used in residential constructions in Catalunya ensure that these components are very airtight.
- The relation between the flue flow coefficient (c_{flue}) and the total flow coefficient (c_1), *Y* (Eq. 2.52) was assumed to be 0.2, which is a typical value (Walker & Wilson, 1998).
- A heavily shielded terrain, many large obstructions within one building height (Walker & Wilson, 1998) was assumed as the shelter situation for the building. The flue was considered unsheltered.
- Dwellings with more than three stories were modeled as three-story buildings.

To calculate the temperature difference, an indoor temperature of 20 ^{o}C was assumed for winter, spring and autumn and 25 ^{o}C for summer. Geographical distribution of the *ACH* obtained by census tract for each season under average meteorological conditions and extreme conditions are shown in Figure 4.14 and Figure 4.15. Highest *ACH* belong to winter, followed by spring, autumn and summer. This behavior is directly related to the severity of meteorological conditions, as was expected, since more drastic meteorological conditions (temperature difference and wind speed) induce higher infiltration airflow. Geographically, higher *ACH* are located in the north-west while smaller belong to the coastline.

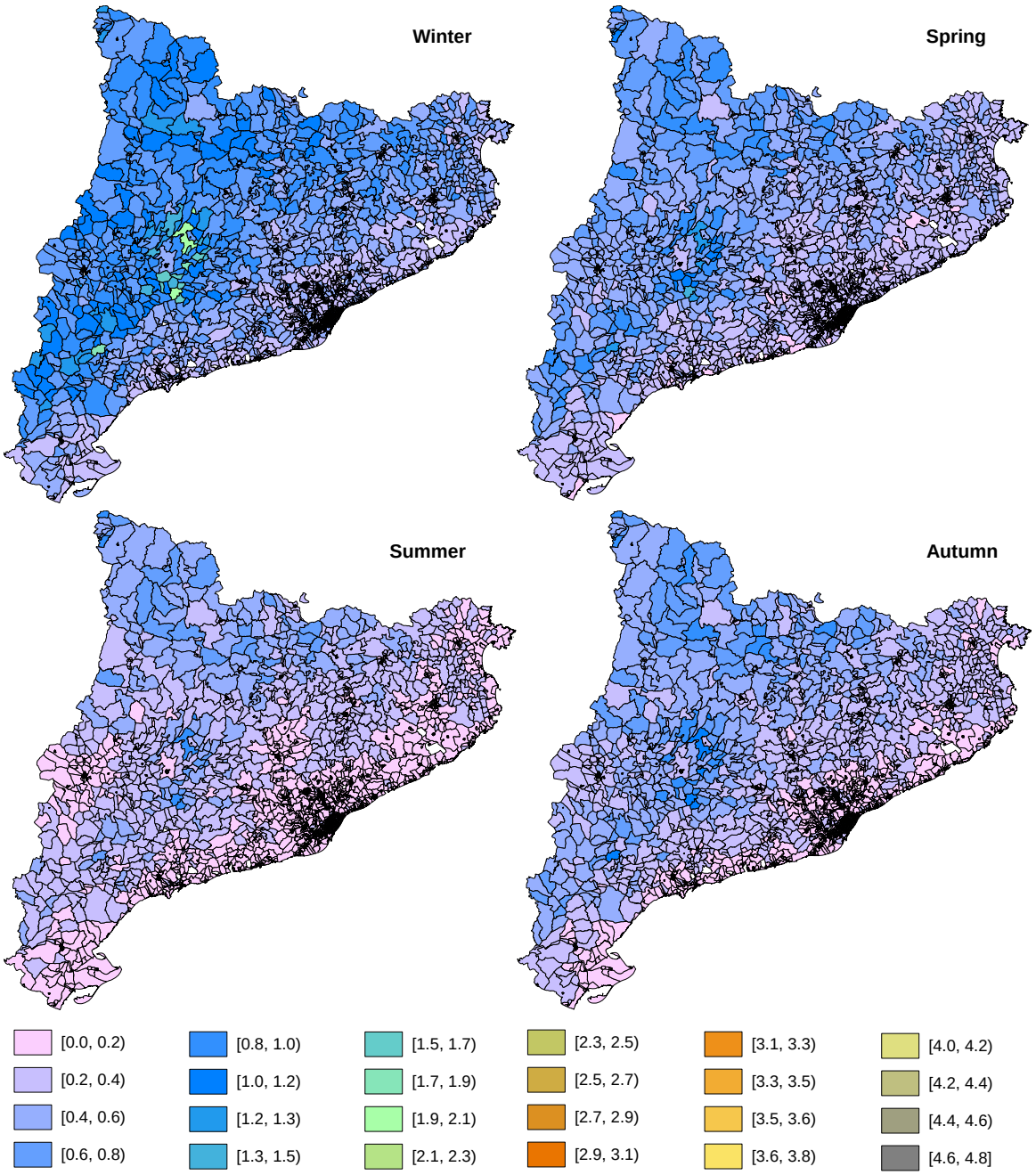

Figure 4.14 Distributions of the *ACH* for average meteorological conditions obtained using the geometric means of dwellings' characteristics by census tract

Figure 4.16 and Figure 4.17 show the cumulative distributions of these *ACH* for average and extreme meteorological conditions, respectively. We can see that for average meteorological conditions, in winter the *ACH* lays around 0.3 and 1 h^{-1}, in spring between 0.2 and 0.8 h^{-1}, in autumn between 0.1 and 0.6 h^{-1}, and in summer between 0.1 and 0.4 h^{-1}. Concerning the *ACH* for extreme meteorological conditions, a similar behavior to that of the average conditions was found. In this case, *ACH* for winter remains between 0.5 and 1.4 h^{-1}, for spring between

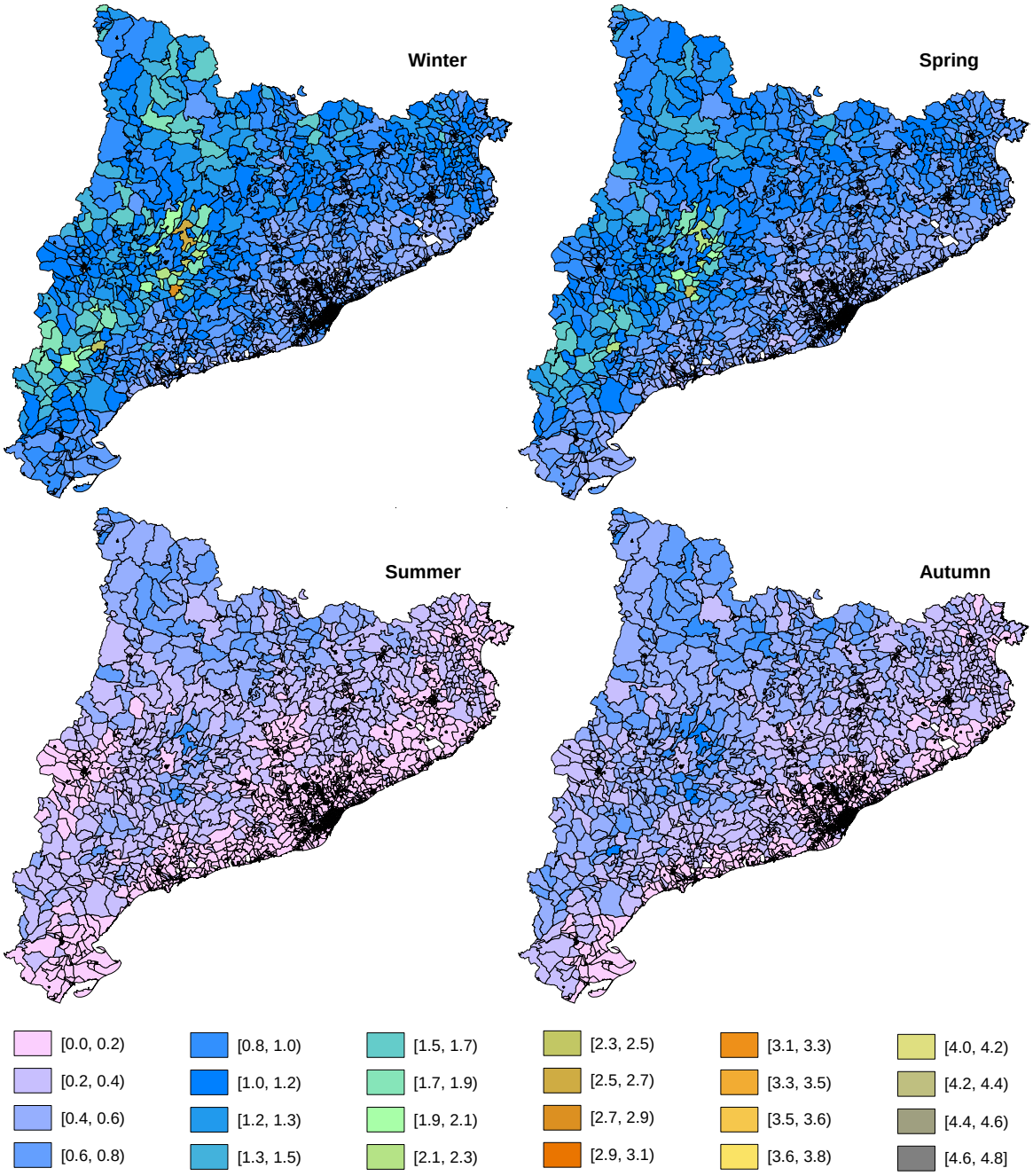

Figure 4.15 Distributions of the *ACH* for extreme meteorological conditions obtained using the geometric means of dwellings' characteristics by census tract

0.4 and 1h^{-1}, for autumn between 0.4 and 0.9 h^{-1}, and for summer between 0.3 and 0.7 h^{-1}. With regards to average meteorological conditions, *ACH* for extreme conditions increased by around 0.3 h^{-1}.

In comparison with the *ACH* statistics in the US, presented in Table 2.17, we can say that *ACH* distributions in Catalunya for average meteorological conditions (Figure 4.16) are lower than those of the US. In addition, we can also see that the amplitude of the distributions for

summer, spring and autumn is very narrow, which might be a consequence of the use of geometric means for dwellings characteristics instead of calculating the *ACH* for each dwelling, generating a loss of information regarding minimum and maximum values of dwellings' characteristics.

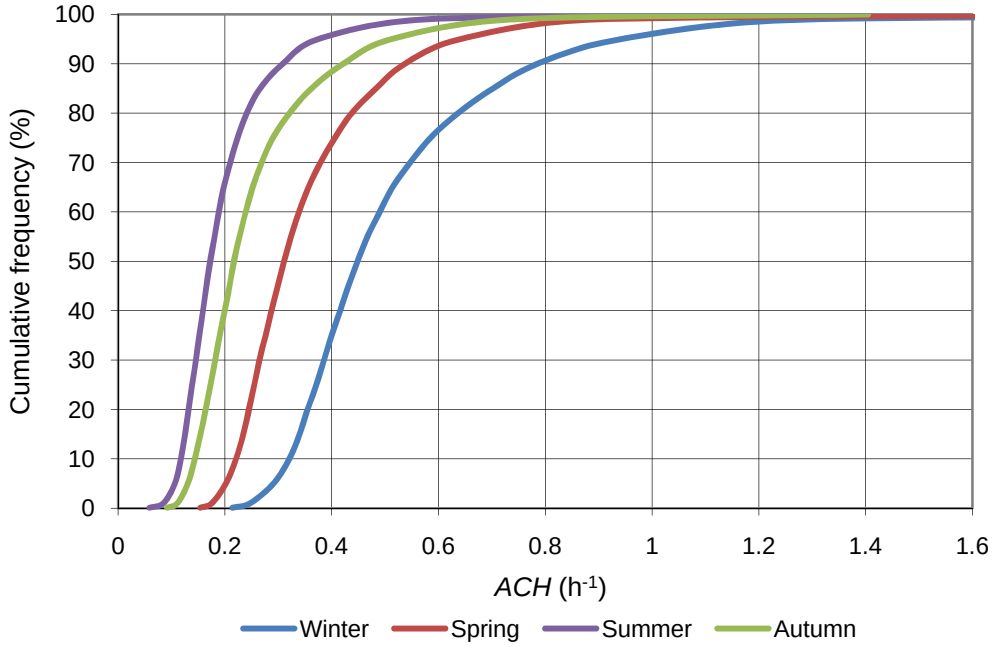

Figure 4.16 Cumulative distributions of the *ACH* for average meteorological conditions obtained using the geometric means of dwellings' characteristics by census tract

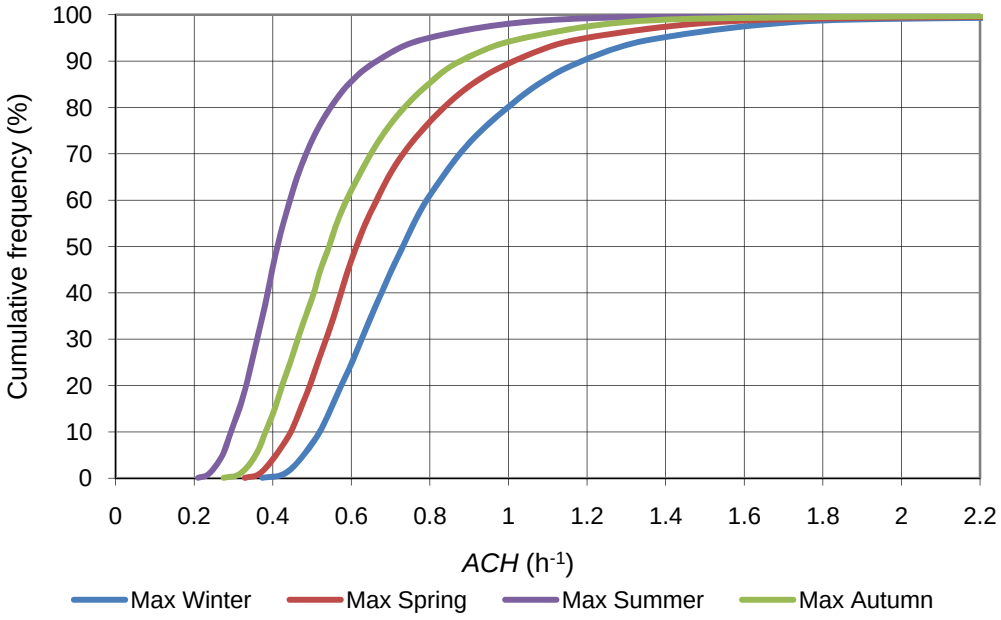

Figure 4.17 Cumulative distributions of the *ACH* for extreme meteorological conditions obtained using the geometric means of dwellings' characteristics by census tract

4.3.2 Using stochastic simulation

A stochastic simulation mimics or replicates the behavior of a system, by exploiting randomness to obtain statistical sample of possible outcomes. This method is useful to study non-deterministic processes, deterministic systems that are too complicated to model analytically or deterministic problems whose high dimensionality makes standard discretizations infeasible (Heath, 2002). The estimation of the airtightness of each dwelling in Catalunya is a deterministic problem, where the discrete probabilities of the variables (floor area, year of construction and number of stories) are known by census tract, but the lack of information concerning the joint probability of the variables to establish the exact characteristics of each dwelling, makes it very complicated to model it analytically. Therefore, we performed a stochastic simulation in order to obtain random building characteristics for every dwelling inside each census tract (Heath, 2002), which represent the real discrete probability distribution of the variable by census tract (see Annex A for an example of the discrete probability distribution). Then, in order to estimate the airtightness, we applied the LBNL airtightness model and finally, through Eq. 4.2 the flow coefficient was computed for every dwelling in each census tract. For the Age variable, we estimated the age of the dwellings up to year 2008. Figure 4.18 describes the steps followed in the application of the stochastic simulation to estimate the airtightness of each dwelling. This procedure was applied to census tracts with more than 10 dwellings, and the number of data simulated was equal to the number of single-family dwellings in each census tract. All the calculations were implemented into a code program developed in Matlab 7 (2009) (see Annex B for the description of the codes used).

Since the aim of the stochastic simulation is to obtain statistical samples of possible results for a variable, it is expected that when applied to the same population, the results obtained follow a similar distribution independently on the number of stochastic simulations performed. Thus, in order to determine if there was any significant difference between the predicted distributions of c obtained with different stochastic simulations for the same census tract, we developed two tests. First, we determined the number of simulations required to obtain a constant cumulative average of c for a sample of census tracts with different number of dwellings (Eq. 4.3). The criterion used in this case was that the difference between actual (r) and previous (r-1) cumulative average were lower than 1%. Second, we performed an analysis of variance of the predicted distributions for each census tract of the sample.

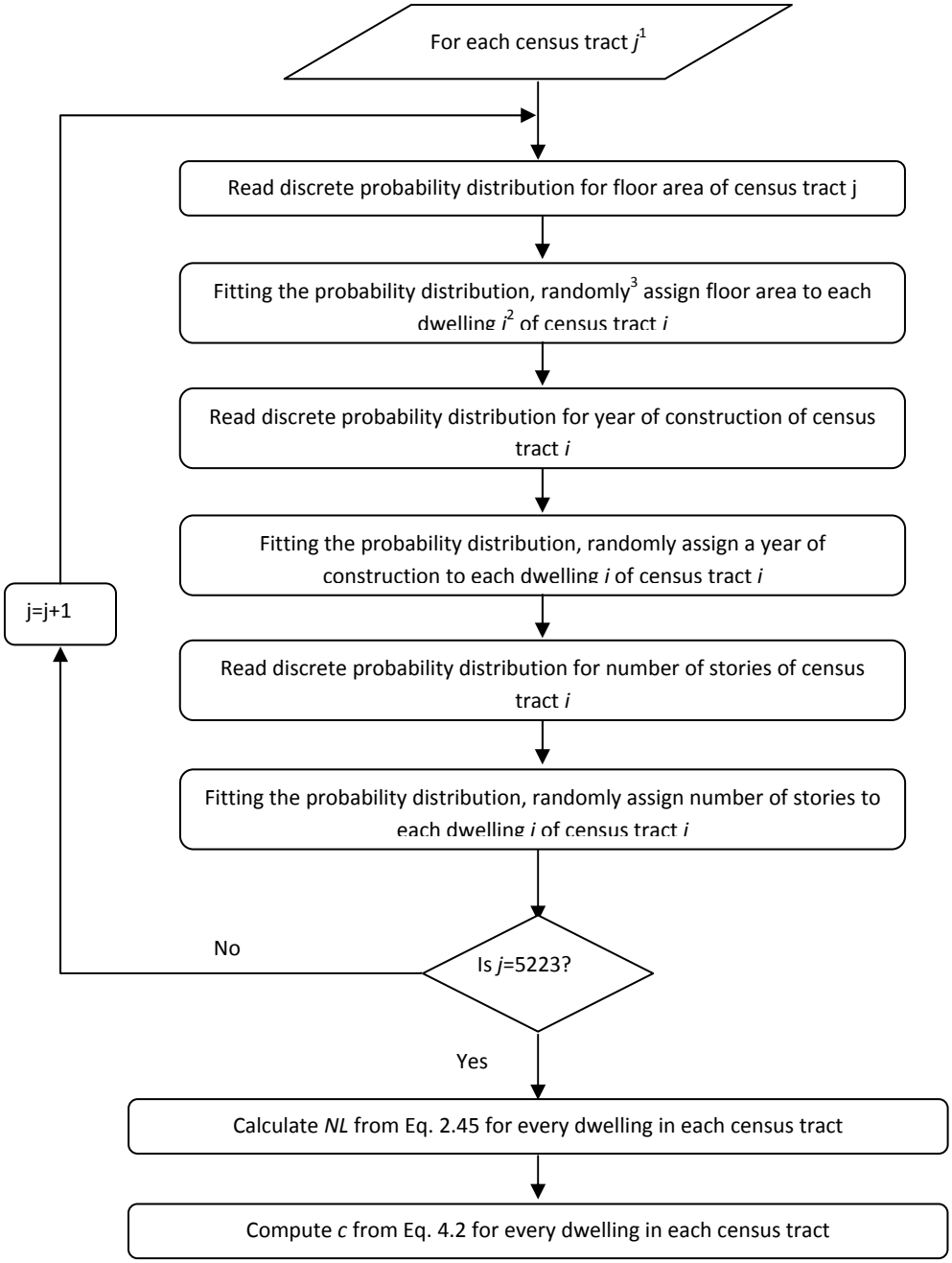

[1] *j* denotes the number of census tracts

[2] *i* denotes the number of dwellings in census tract j

[3] Assignation of random values was done using the random function of Matlab

Figure 4.18 Schematic diagram for the airtightness estimation using the stochastic simulation

$$c = \frac{\sum_{r=1}^{N\ simulations} \sum_{i=1}^{N\ dwellings} c_{r,i}}{r \cdot i} \qquad \text{Eq. 4.3}$$

Table 4.2 shows the results for the first test, where we can observe that there is no relation between the required number of simulations and the number of dwellings of the census tract. Also, we can see that it requires around 2 to 14 simulations to fulfill the criterion.

Table 4.2 Required simulations to obtain a constant cumulative average

Number of dwellings	Section	Number of simulations	Number of dwellings	Section	Number of simulations
10	801509044	6	180	807601002	8
20	801503002	12	200	818707001	8
30	801507015	5	250	812601001	3
40	801507005	4	300	813601005	3
50	801507010	7	400	820002013	3
60	800801001	4	499	4313701001	5
70	801907188	10	599	804201001	6
80	801907067	4	699	4302801001	2
90	810201001	13	792	820505001	3
100	810201001	4	902	823401001	3
120	801502001	6	967	829101001	3
140	800902002	4	1648	802301001	5
160	256101001	2			

In addition to the estimation of the average value of *c* by simulation and the cumulative average, we also estimated the standard deviation and the 10^{th}, 50^{th} and 90^{th} percentiles of the cumulative distribution for each simulation by census tract. Little variation was observed for these indicators within simulations (results of these simulations are shown in Annex C). In the second test, we determined whether the predicted distribution of *c* varied within simulations. As the maximum number of simulations required to obtain a constant cumulative average was 14, we decided to fix the number of simulations to 20, a higher value so that we assure no bias of the distributions. From the results obtained (Table 4.3), not all the predicted distributions of *c* followed a log-normal distribution, however, a trend concerning the distributions for census tracts with less numbers of dwellings is observed, being these tracts the ones that generally fit the log-normal distribution. As not all the predictions fit the log-normal distribution, we evaluated the variability between groups by applying the Kruskal-Wallis test, which is a non-parametric method for the analysis of variance in data that do not follow a given probability distribution (Montgomery, 2007). Results of theses test (see Annex C) showed *P*-values higher than 0.05, which reject the hypothesis of any significant difference between the medians of *c* with 95% confidence for each of the census tracts analyzed. Additionally, box plots were drawn for each simulation by census tract; where very little variation among the 25^{th}, 50^{th} and 75^{th} percentiles was observed, remarking the resemblance of the distributions.

Table 4.3 Number of simulations that fit a log-normal distribution based on Lilliefors' test

Number of dwellings	Yes	No	Number of dwellings	Yes	No
10	20	0	180	5	15
20	19	1	200	3	17
30	20	0	250	12	8
40	20	0	300	17	3
50	19	1	400	0	20
60	16	4	499	0	20
70	20	0	599	1	19
80	19	1	699	0	20
90	15	5	792	0	20
100	20	0	902	0	20
120	5	15	967	0	20
140	19	1	1648	0	20
160	15	5			

The cumulative distribution of *ELA* obtained using this model is shown in Figure 4.19, where we can see that 80% of the dwellings exhibit *ELAs* lower than 0.1m^2 and 17% between 0.1 and 0.2 m^2. Typical values of *ELA* for single-family dwellings in the US range from 0.04 m^2 (tight) to 0.3 m^2 (leaky) (Chan *et al*., 2005), if we take these values as reference, we can see that predicted *ELA*s fall into the same range but are closer to the lower value.

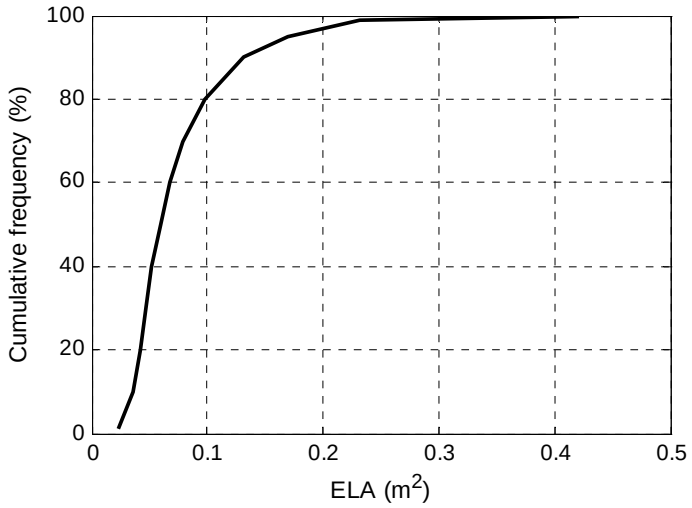

Figure 4.19 *ELA* cummulative distribution of Catalan single-family dwellings obtained with the LBNL model

Figure 4.20 and Figure 4.21 show the geometric mean of the *ACH* obtained for each census tract across Catalunya using the stochastic simulation. These figures present higher *ACH* than those of Figure 4.14 and Figure 4.15 as was expected since they consider the whole distribution instead of central values for dwellings characteristics. Principal differences appear

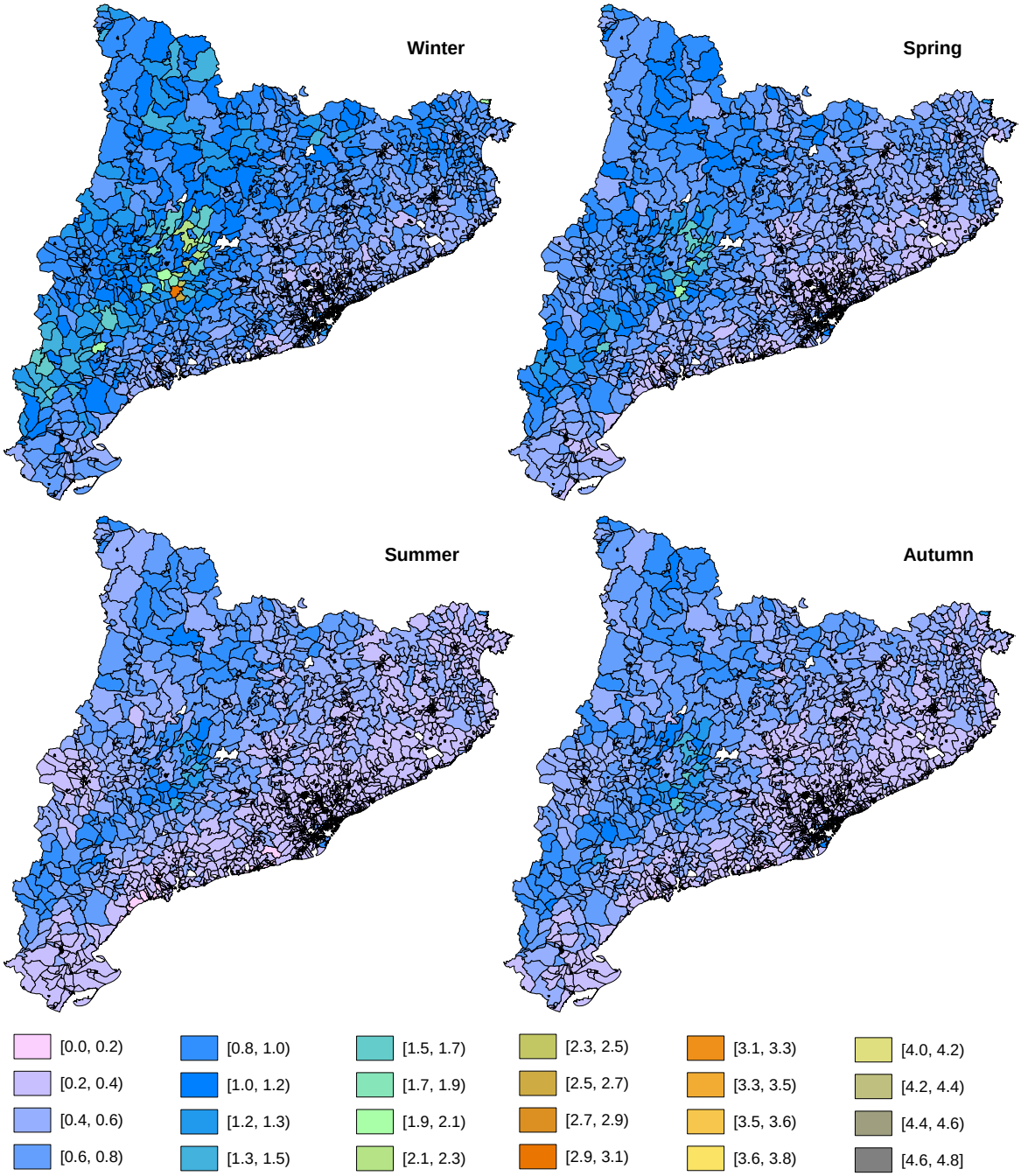

Figure 4.20 Geometric means of *ACH* for average meteorological conditions by census tract obtained using the stochastic simulation.

in the case of extreme conditions, where most of the census tracts exhibit *ACH* above 0.6 h^{-1} and highest values reached around 7 h^{-1} in comparison with Figure 4.15 where almost all the *ACH* were below 1.6 h^{-1}.

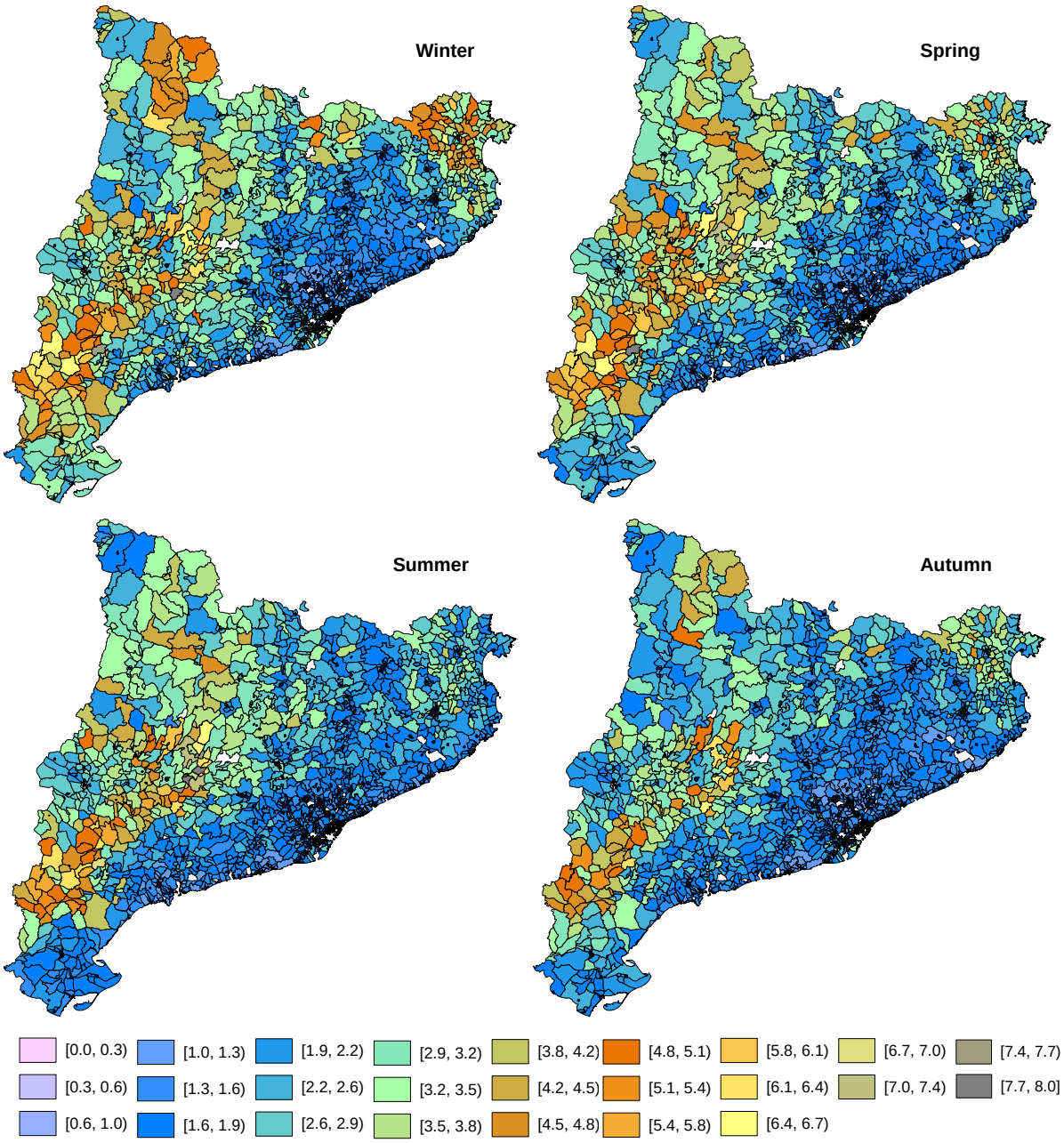

Figure 4.21 Geometric means of *ACH* for extreme meteorological conditions by census tract obtained using the stochastic simulation.

Figure 4.22 and Figure 4.23 show the cumulative distributions of *ACH* obtained using the stochastic simulation for average and extreme meteorological conditions, respectively. Here we can see that averages meteorological conditions in winter stay around 0.3 and 1.4 h^{-1}, in spring between 0.2 and 1.2 h^{-1}, in autumn between 0.15 and 1 h^{-1}, and in summer between 0.15 and 1 h^{-1} (using the 10^{th} and 95^{th} percentiles). Concerning the *ACH* for extreme meteorological conditions, higher values with respect to those of average conditions were found, showing an important difference. In this case, *ACH* for winter remain between 1 and 6

h^{-1}, for spring between 1.5 and 5 h^{-1}, for autumn between 1 and 4.5 h^{-1}, and for summer 1 and 4.5 h^{-1}. In addition, it is interesting to see that for extreme conditions, *ACH* for autumn were a little bit lower than those of summer, which is also different from the behavior of distributions shown in Figure 4.17, were lowest *ACH* belong to summer.

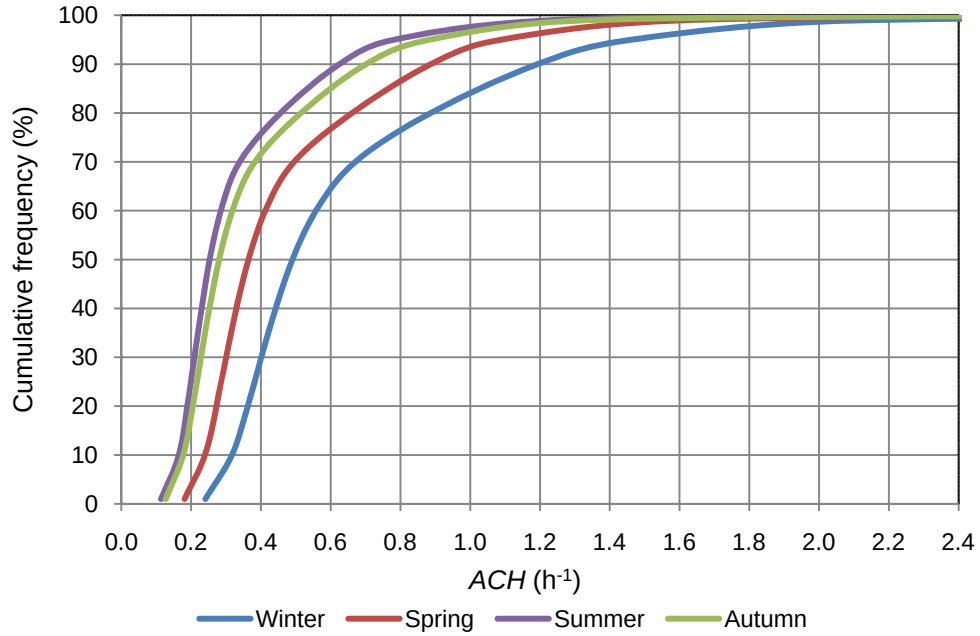

Figure 4.22 Cumulative distribution of *ACH* for average meteorological conditions using the stochastic simulation by census tract

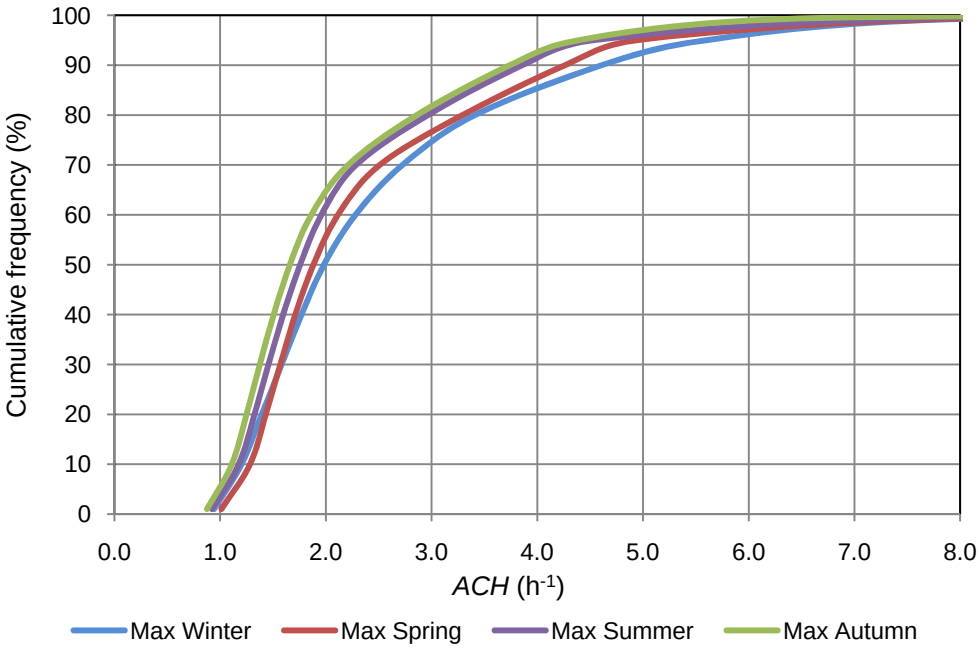

Figure 4.23 Cumulative distribution of *ACH* for extreme meteorological conditions using the stochastic simulation by census tract

Concerning the difference between the predictions made with the geometric means for dwellings characteristics and the stochastic simulations, wider ranges of *ACH* were obtained in the last case, as was expected since it covers all the range of variability of dwellings characteristics. The influence of this fact is more noticeable in the case of extreme conditions where the range of *ACH* passed from 0.2-2 h^{-1} (Figure 4.17) for geometric means to values between 1 and 8 h^{-1} (Figure 4.23) with the stochastic simulation, with 60% of the dwellings staying among 1 and 2 h^{-1} and less than 1% under 0.8 h^{-1}.

From these results we can say that the application of the LBNL airtightness model to Catalan single-family dwellings gave an approach of the airtightness distribution. However the *NL* obtained is highly affected by the climate zone distribution, pointing out that census tracts located in dry climate zone are less airtight and consequently leakier. This might not be the case for Catalunya, and a more homogeneous distribution is expected, since differences in construction quality or materials among the different regions of Catalunya are negligible.

Also, the difference in constructions techniques, dwellings typology and model parameters specific for a climate zone between Catalunya and the US, may affect the airtightness prediction of Catalan dwellings. Therefore, it would be more appropriate to develop a model based on Spanish infiltration measurements, but since there is no data available, leakage data of French dwellings is the best option to develop a model that could resemble more to Catalunya, due to the similarities between French and Catalan dwellings and to climate in both countries.